Lithium Insertion Mechanism in Tin-Based Spinel Sulfides

C. Branci,* J. Sarradin, J. Olivier-Fourcade, and J. C. Jumas

Laboratoire de Physicochimie de la Matière Condensée (UMR C5617 CNRS), Université Montpellier II, Place Eugène Bataillon, 34095 Montpellier Cedex 5, France

Received April 12, 1999. Revised Manuscript Received May 20, 1999

$Cu_2MSn_3S_8$ (M = Fe, Co) spinel compounds have been studied as cathode materials in Li/$LiPF_6$(1M)-PC-EC/spinel sulfide cells. To understand the lithium insertion mechanism, both pristine compounds and chemically inserted products were characterized by X-ray Powder Diffraction (XPD), ^{119}Sn Mössbauer Spectroscopy (MS), and X-ray Absorption Spectroscopy (XAS) at the sulfur K-edge. To accommodate the inserted lithium ions, two steps of reduction have been observed. First, for a low lithium content (up to 2 Li per formula), a copper reduction is occurring. Moreover, for the iron-based compound the copper atoms extraction is associated with a migration of iron atoms from the 16c octahedral sites toward the 8a tetrahedral sites. Second, for a high lithium content (above 2 Li per formula) a complex and simultaneous reduction of tin(IV) toward tin(II) and tin(0) has been clearly observed as well as a distortion of sulfur coordination polyhedra during the insertion process. From an electrochemical point of view, these spinels are rather interesting as model compounds regarding the lithium insertion study.

Introduction

The principle of using $A[B_2]X_4$ spinel as a stable host structure for anodes and cathodes in rechargeable lithium cells was demonstrated several years ago.[1−2] Indeed, the occurrence of a nonnegligible number of empty sites in this framework is particularly favorable to guest ions. Since the report of Eisenberg,[3] chalcogenide spinels have proven adequate candidates for electrodes materials in lithium and "Lithium-ion" batteries.[4−8] Despite a very weak tetragonal distortion distinguishable by detailed single-crystal X-ray analysis,[9] the compounds with $Cu_2MSn_3S_8$ (M = Fe, Co) stoichiometry can be described in the $Fd\bar{3}m$ space group. These cubic normal spinels $Cu_2MSn_3S_8$ have a three-dimensional lattice with Cu(I) cations occupying the 8a tetrahedral sites, while M(II) and Sn(IV) cations are randomly distributed in 16d octahedral sites and the sulfur anions in a close packed (ccp) arrangement. Thus, the 16c octahedral and 8b and 48f tetrahedral interstices are empty and available for lithium intercalation.

Recently,[10] the electrochemical behavior of the $Cu_2MSn_3S_8$ compounds with Li ranging from 0 to 2 per formula has been reported but the lithium insertion process is not precisely known. The cobalt-based compound has been studied as an anodic material in "lithium-ion" cells associated with $LiCoO_2$[11] as cathodic material. Copper extraction was also performed to improve the electrochemical behavior by the presence of vacancies in 8a sites.

To study the insertion process, several methods of characterization have been performed in this research. The lithium insertion was carried out in a chemical manner via a reducing agent (*n*-butyllithium). First of all, the purity of pristine compounds and the crystallinity state of lithiated samples were checked by X-ray diffraction. In a second step, the local environment of tin and sulfur atoms was studied by ^{119}Sn Mössbauer Spectroscopy (MS) and X-ray Absorption Spectroscopy (XAS) at the sulfur K-edge, respectively. Finally, the conduction properties of these compounds have been investigated.

Experimental Section

Spinel compounds have been synthesized by the solid-state reaction from pure elements, mixed, and sealed in evacuated quartz tubes ($P = 10^{-3}$ Pa). The mixtures were heated at 300 °C, at 50 °C/h. The temperature was kept constant for 1 day. The temperature was then raised to 750 °C and maintained at this value for 10 days. The black powder obtained was ground and stored in an argon-filled glovebox.

Chemical lithium insertion was carried out by the *n*-butyllithium technique.[12] The sulfide powder was suspended

(1) Thackeray, M. M.; Goodenough, J. B. U.S. Patent, 44,507,371, 1985.
(2) Thackeray, M. M.; Johnson, P. J.; de Picciotto, L. A.; Bruce, P. G.; Goodenough, J. B. *Mater. Res. Bull.* **1984**, *19*, 179.,
(3) Eisenberg, M. *J. Electrochem. Soc.* **1980**, *127*, 2382.
(4) James, A. C. W. P.; Goodenough, J. B.; Clayden, N. J. *J. Solid State Chem.* **1988**, *77*, 356.
(5) Thackeray, M. M. *J. Electrochem. Soc.* **1995**, *142* (8), 2558.
(6) Pistoia, G.; Zane, D.; Zhang, Y. *J. Electrochem. Soc.* **1995**, *142* (8), 2551.
(7) Elidrissi Moubtassim, M. L.; Bousquet, C.; Olivier-Fourcade, J.; Jumas, J. C.; Tirado, J. L. *Chem. Mater.* **1998**, *10*, 968.
(8) Morales, J.; Tirado, J. L.; Elidrissi-Moutbassim, M. L.; Olivier-Fourcade, J.; Jumas, J. C. *J. Alloys Compounds* **1995**, *217*, 176.
(9) Jumas, J. C.; Philippot, E.; Maurin, M. *Acta Crystallogr.* **1980**, *B36*, 1993.
(10) Lavela, P.; Tirado, J. L.; Morales, J.; Olivier-Fourcade, J.; Jumas, J. C. *J. Mater. Chem.* **1996**, *6* (1), 41.
(11) Cochez, M. A.; Jumas, J. C.; Lavela, P.; Morales, J.; Olivier-Fourcade, J.; Tirado, J. L. *J. Power Sources* **1996**, *62*, 99.
(12) Thackeray, M. M.; David, W. I. F.; Goodenough, J. B. *Mater. Res. Bull.* **1982**, *17*, 1307.

10.1021/cm991049a CCC: $18.00
Published on Web 09/15/1999

in a 1.5 M solution of (n-C_4H_9)Li in hexane. The temperature of the reaction was maintained constant at 35 °C and an experimental set was kept under dry argon during the reaction. The inserted sample was then collected, filtered, washed with hexane, and stored in an argon-filled glovebox to avoid oxidation reactions. The determination of the amount of inserted lithium was performed by atomic emission spectroscopy using a Philips (Pye Unicam SP9) spectrometer. The experimental details of the measurements were previously reported.[13]

X-ray diffraction diagrams, recorded on a Philips diffractometer using Cu Kα radiation, have been used to characterize the compounds before and after lithium intercalation. For the lithiated samples, a plastic film was used to avoid the undesirable oxidation reactions occurring with air during the recording of the patterns. The local environment of tin atoms was studied by means of ^{119}Sn MS. The spectra were obtained at room temperature using an Elscint Ame 40 constant acceleration spectrometer. The γ-ray source was ^{119m}Sn in a $BaSnO_3$ matrix. The velocity scale was calibrated by using a ^{57}Co source and the magnetic sextuplet of a high purity iron foil absorber. The spectra were fitted to Lorentzian profiles by a least-squares method[14] and the quality of fit was controlled by classical X^2 tests. All the isomer shifts reported are given with respect the center of a $BaSnO_3$ spectrum obtained from the same source.

The XAS measurements at the sulfur K-edge were recorded using the synchrotron radiation of Super ACO storage ring at LURE (Orsay, France). The samples to be investigated were finely ground and passed through a 5 μm sieve in order to obtain powders being homogeneous in particle size. Then the powder was spread on adhesive tape fixed to an aluminum plate. Two parallel Si(111) crystals were used as monochromators and yielded a resolution of 0.4 eV. The absorption spectra were corrected for a linear baseline which was fitted to the preedge part of each spectrum. Finally, the spectra were normalized between 0 and 1.

The conductivity measurements were performed in an evacuated Pyrex chamber, connected to an impedance analyzer (HP 4192 A) driven by a computer.

Results and Discussion

The indexation of XPD patterns (Figure 1) of the pristine compounds in $Fd\bar{3}m$ space group of a cubic spinel confirms the purity of the phases obtained by direct synthesis. The XPD patterns of the chemically lithiated samples were already reported.[10] A gradual decrease of the diffraction peaks intensity appears as a consequence of a progressive structure amorphization depending on the amount of intercalated lithium. An analysis of these patterns showed a very weak line attributable to copper metal and due to de-intercalation of reduced copper. For both compounds, the lithium intercalation gives rise to an extration of copper atoms from the 8a sites. Moreover, concerning the $Li_xCu_2FeSn_3S_8$ compound the ^{57}Fe MS has shown a migration of iron atoms from 16d to 8a sites, simultaneously to the copper extraction.[15] To get a better understanding of the lithium insertion mechanism, some additional characterizations were performed using XAS study at the sulfur K-edge and ^{119}Sn MS.

The ^{119}Sn Mössbauer spectra are presented Figure 2 and the hyperfine parameters are listed Table 1. For the pristine compounds, the isomer shifts (1.246(3) and

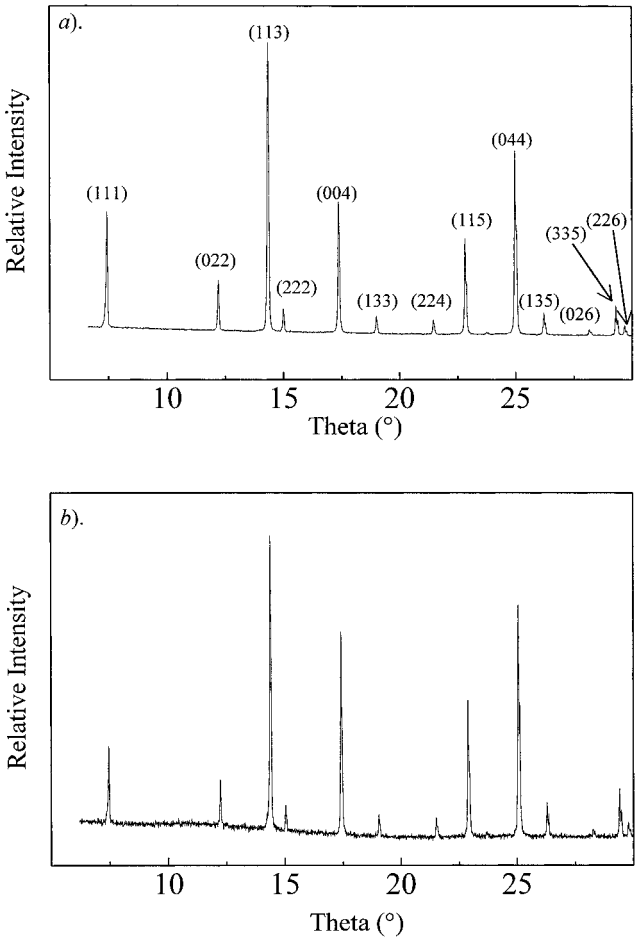

Figure 1. XPD patterns of pristine samples: (a) $Cu_2FeSn_3S_8$ and (b) $Cu_2CoSn_3S_8$.

1.211(4) mm/s) are characteristic of tin with an oxidation state (IV) in a slightly distorted octahedral environment. This result agrees with those previously published.[16] The distorted environment can be explain by the occurrence of second neighbors (M(II) and Sn(IV)) randomly distributed around the tin atoms. With regard to the lithiated samples, the same behavior is observed for both compounds, and the process can be divided in two steps. During the first step (0−2.3 and down from 4.2 Li per formula for $Cu_2FeSn_3S_8$ and $Cu_2CoSn_3S_8$, respectively), no additional signal is observed in the spectra. The insertion of lithium ions occurs without reduction of tin atoms. During the second step (above 2.3 Li per formula for $Cu_2FeSn_3S_8$ and 4.2 Li per formula for $Cu_2CoSn_3S_8$), two subspectra appear (Figure 3) with isomer shifts corresponding to tin atoms associated with lower oxidation states (Sn(II) $2.99 < \delta < 3.15$ and Sn(0) $2.23 < \delta < 2.7$). To confirm this reduction process, a measurement at 80 K was performed. In fact, the difference between the tin(IV) and tin(II) Lamb−Mössbauer factor (part of probed atoms which absorbed γ-ray recoilless) is more important at low temperature.[17] Indeed, in this range of temperature the region of the spectrum included between 2 and 3.5 mm/s is better defined. Both spectra at 80 K and at room temperature

(13) Elidrissi-Moutbassim, M. L.; Olivier-Fourcade, J.; Senegas, J.; Jumas, J. C. *Mater. Res. Bull.* **1993**, *28*, 1083.
(14) Kundig, W. *Nucl. Instrum. Methods* **1979**, *75*, 336.
(15) Branci, C.; Sarradin, J.; Olivier-Fourcade, J.; Jumas, J. C. *J. Power Sources.* **1999**, accepted for publication.
(16) Padiou, J.; Jumas, J. C.; Ribes, M. *Rev. Chim. Miner.* **1981**, *18*, 33.
(17) Gonser, U. *Microscopic Methods in Metals*; 410 ed.; Gonser, U. Ed.; Springer-Verlag: Berlin, 1989.

Table 1. Hyperfine Parameters of ^{119}Sn Mössbauer Spectra of $Li_xCu_2FeSn_3S_8$ and $Li_xCu_2CoSn_3S_8$ at Different *x* Values[a]

compound	composition (*x*)	IS (mm/s)	QS (mm/s)	LW (mm/s)	attribution	X^2 test
$Li_xCu_2FeSn_3S_8$	0	1.246(3)	0.367(7)	1.066(6)	Sn(IV)	0.488
	0.7	1.233(7)	0.25(1)	0.94(1)	Sn(IV)	0.566
	2.3	1.246(2)	0.314(4)	0.938(4)	Sn(IV) − 95%	0.576
		2.4(2)	1.5(3)	0.90(8)	Sn(0) − 2%	
		3.0(1)	0.90(8)	0.90(8)	Sn(II) − 3%	
	6	1.252(5)	0.287(8)	0.941(7)	Sn(IV) − 71%	0.478
		2.62(2)	1.23(3)	0.9(1)	Sn(0) − 12%	
		3.11(1)	0.90(2)	0.95(3)	Sn(II) − 16%	
	7	1.281(7)	0.34(1)	0.86(1)	Sn(IV) − 68%	0.359
		2.66(2)	1.08(2)	0.76(4)	Sn(0) − 17%	
		3.15(2)	0.95(2)	0.76(4)	Sn(II) − 15%	
	7 (at 80 K)	1.466(1)	0.46(1)	0.95(1)	Sn(IV) − 48%	0.395
		2.70(3)	1.21(3)	0.95(3)	Sn(0) − 20%	
		3.15(1)	0.96(2)	0.95(3)	Sn(II) − 32%	
$Li_xCu_2CoSn_3S_8$	0	1.211(4)	0.359(7)	1.096(7)	Sn (IV)	0.628
	1.2	1.195(4)	0.298(7)	1.022(6)	Sn(IV)	0.522
	4.2	1.173(5)	0.303(7)	0.873(7)	Sn(IV) − 73%	0.506
		2.23(1)	1.42(3)	0.93(7)	Sn(0) − 15%	
		2.99(2)	0.96(4)	0.93(7)	Sn(II) − 12%	
	5.6	1.154(6)	0.274(9)	0.894(8)	Sn(IV) − 65%	0.440
		2.27(6)	1.37(2)	0.89(5)	Sn(0) − 20%	
		3.00(2)	0.96(1)	0.89(5)	Sn(II) − 15%	
	6.2	1.14(1)	0.29(2)	0.94(3)	Sn(IV) − 61%	0.483
		2.26(1)	1.35(2)	0.97(2)	Sn(0) − 17%	
		3.05(2)	0.90(4)	0.97(2)	Sn(II) − 22%	

[a] Abbreviations: IS, isomer shift; QS, quadrupole splitting, and LW, full-width at half maximum.

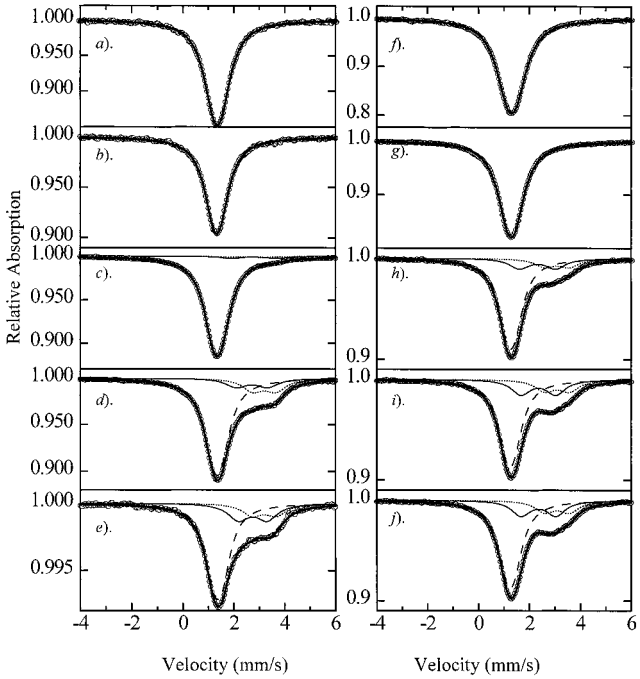

Figure 2. ^{119}Sn Mössbauer spectra of pristine and lithiated phases: (a) $Cu_2FeSn_3S_8$, (b) $Li_{0.7}Cu_2FeSn_3S_8$, (c) $Li_{2.3}Cu_2FeSn_3S_8$, (d) $Li_6Cu_2FeSn_3S_8$, (e) $Li_7Cu_2FeSn_3S_8$, (f) $Cu_2CoSn_3S_8$, (g) $Li_{1.3}Cu_2CoSn_3S_8$, (h) $Li_{4.2}Cu_2CoSn_3S_8$, (i) $Li_{5.6}Cu_2CoSn_3S_8$, and (j) $Li_{6.2}Cu_2CoSn_3S_8$.

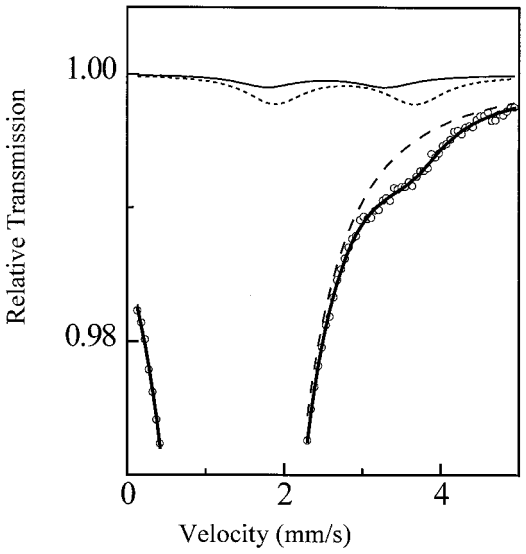

Figure 3. Zoom in the ^{119}Sn Mössbauer spectrum of $Li_{2.3}Cu_2FeSn_3S_8$.

are presented Figure 4. The corresponding hyperfine parameters are listed in Table 1. The result obtained at 80 K confirms the occurrence of two doublets on the right of the subspectrum corresponding to Sn(IV). The slight difference obtained in the isomer shift calculated at 80 K and room temperature is mainly due to a Döppler effect of second order.

A complex and simultaneous reduction Sn(IV) → Sn(II), Sn(0) occurs above 2 inserted lithium per formula. The ratio of reduced tin increases with the amount of intercalated lithium. This complex reduction was previously observed with $Li_xCu_2FeSn_3S_8$[18] and SnS_2[19] compounds.

The sulfur environment was studied by means of X-ray absorption measurements at the sulfur K-edge. The lithiated and pristine spectra are presented Figure 5. With regard to the pristine compounds, a comparison between these quaternaries and some binaries (SnS_2 and FeS) allowed to attribute the electronic transitions[20] for the three features labeled 1, 2. and 3 in Figure 5. The main absorption, 1, has been attributed to the

(18) Branci, C.; Sarradin, J.; Olivier-Fourcade, J.; Jumas, J. C. *Mol. Cryst. Liq. Cryst.* **1998**, *311*, 69.
(19) Olivier-Fourcade, J.; Jumas, J. C.; Womes, M.; Lavela, P.; Tirado, J. L.; Morales, J. *Conf. Proc. ICAME 95* **1996**, *50*, 75.
(20) Branci, C.; Womes, M.; Lippens, P. E.; Olivier-Fourcade, J.; Jumas, J. C. *J. Solid State Chem.* **1998**, submitted for publication.

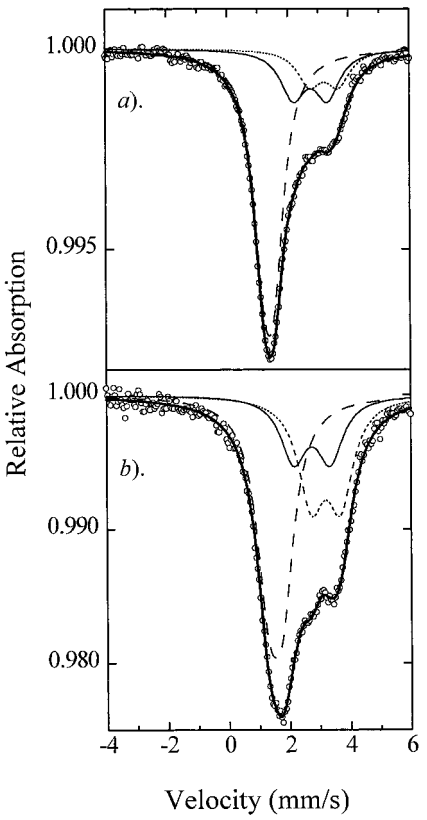

Figure 4. ^{119}Sn Mössbauer spectra of $Li_7Cu_2FeSn_3S_8$ at (a) room temperature and (b) 80 K.

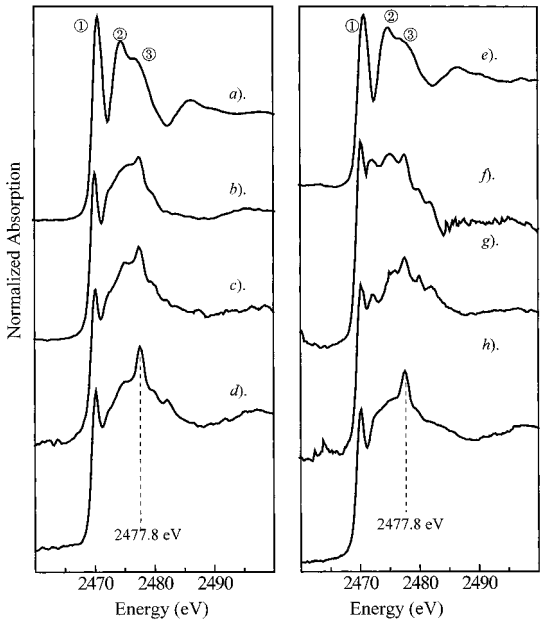

Figure 5. X-ray absorption spectra at S K-edge of (a) $Cu_2FeSn_3S_8$, (b) $Li_{0.7}Cu_2FeSn_3S_8$, (c) $Li_{2.3}Cu_2FeSn_3S_8$, (d) $Li_6Cu_2FeSn_3S_8$, (e) $Cu_2CoSn_3S_8$, (f) $Li_{1.3}Cu_2CoSn_3S_8$, (g) $Li_{4.2}Cu_2CoSn_3S_8$, and (h) $Li_{5.6}Cu_2CoSn_3S_8$.

electronic transition S 1s → S 3p − Sn 5s σ*. The second and third features (2 and 3) correspond to the electronic transitions S 1s → S 3p − Sn 5p σ* and S 1s → S 3p − M 4s − M 4p σ* (M = Fe, Co), respectively. These assignments agree well with the theoretical calculation of SnS_2[21] and FeS[22] electronic structure. For the lithiated spectra, important modifications were observed

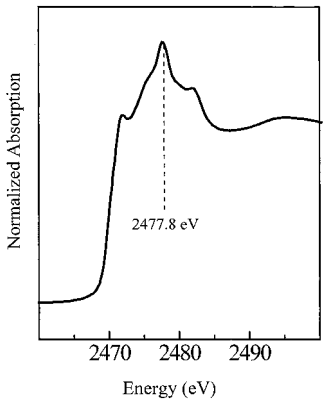

Figure 6. X-ray absorption spectrum at S K-edge of Li_2S.

Table 2. Position and Normalized Absorption of Feature Labeled 1 in Figure 6 for the XAS Spectra at the Sulfur K-edge of $Li_xCu_2FeSn_3S_8$ and $Li_xCu_2CoSn_3S_8$ at Different *x* Values

compound	composition (*x*)	position (eV)	normalized absorption
$Li_xCu_2FeSn_3S_8$	0	2470.6	2.1
0.7	2470.1	1.9	
2.3	2470.2	1.7	
6	2470.2	1.2	
$Li_xCu_2CoSn_3S_8$	0	2470.8	1.7
1.2	2470.2	1.7	
4.2	2470.2	1.4	
5.6	2470.2	1.2	

according to the insertion of lithium ions, and two facts can be clearly noted. First, the decreasing of the main absorption intensity (cf. Table 2) corresponds to an increasing of the 5s electronic density around the tin atoms. This fact can be correlated with ^{119}Sn MS results which show a reduction of tin atoms. Indeed, this reduction gives rise to an increasing of the Sn 5s electrons[21] (Sn(IV), $5s^0$and $5p^0$; and Sn(0), $5s^2$ and $5p^2$). Second, from the beginning of the insertion, a new peak appears at 2477.6 eV. To understand this feature it seems important to recall the interpretations of Li_1TiS_2 XAS spectrum at the sulfur K-edge.[23] Indeed, this spectrum shows a similar peak at 2478 eV. With the aid of a theoretical calculation, the authors suggest a charge transfer between lithium and sulfur atoms with the formation of a "Li−S" bond. The peak at 2477.6 eV could be due to the "Li−S" interaction. To confirm this fact, Li_2S XAS spectrum at the sulfur K-edge was recorded, and it is presented in Figure 6: it shows an important peak at 2478 eV. It seems then reasonable to think that the peak observed at 2477.6 eV in the lithiated quaternaries spectra is principally due to a formation of "Li−S" bonds during the insertion process. This variation can be explained by the perturbation of sulfur owing to the formation of "Li−S" bonds.

The conduction properties were checked out by complex impedance spectroscopy. The pristine compounds have a semiconductor behavior. From the zero frequency extrapolation of the complex impedance plot, Arrhenius

(21) Lefebvre, I.; Lannoo, M.; Olivier-Fourcade, J.; Jumas, J. C. *Phys. Rev.* **1991**, *44B*, 1004.
(22) Womes, M.; Karnatak, R. C.; Esteva, J. M.; Lefebvre, I.; Allan, G.; Olivier-Fourcade, J.; Jumas, J. C. *J. Phys. Chem. Solids.* **1997**, *58* (2), 345.
(23) Wu, Z. Y.; Ouvrard, G.; Lemaux, S.; Moreau, P.; Gressier, P.; Lemoigno, F.; Rouxel, J. *Phys. Rev. Lett.*. **1996**, *77* (10), 2101.

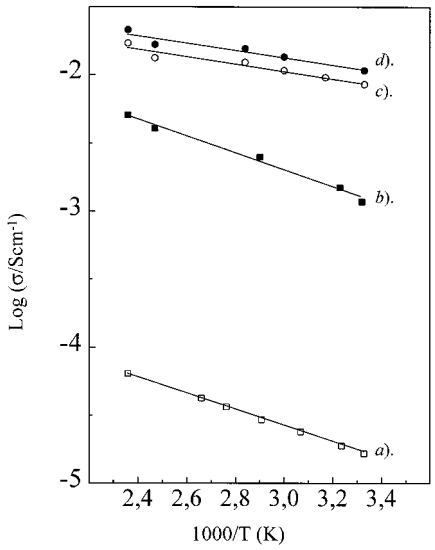

Figure 7. Arrhenius plot of (a) $Cu_2FeSn_3S_8$, (b) $Li_6Cu_2FeSn_3S_8$, (c) $Cu_2CoSn_3S_8$, and (d) $Li_{5.6}Cu_2CoSn_3S_8$.

Table 3. Conductivity at Room Temperature and Activation Energy of $Li_xCu_2FeSn_3S_8$ and $Li_xCu_2CoSn_3S_8$

compound	composition (x)	σ_{RT} (S/cm)	E_a (eV)
$Li_xCu_2FeSn_3S_8$	0	1.6×10^{-5}	0.11
	6	1×10^{-3}	0.12
$Li_xCu_2CoSn_3S_8$	0	8.29×10^{-3}	0.06
	5.6	9.1×10^{-3}	0.05

diagrams were plotted as shown in Figure 7 for both pristine and lithiated compounds. Conductivity values at room temperature of $Cu_2FeSn_3S_8$ and $Cu_2CoSn_3S_8$ are reported in Table 3. At 6 Li per formula, the conductivity value of the iron-based spinel slightly increases since the conductivity at room temperature is equal to 10^{-3} S/cm. This behavior could be explained either by the additional ionic part of the conductivity due to the inserted lithium ion or by the electronic part due to the electron transfer giving rise to a modification of the band structure (Fermi level). Only a detailed study of the conduction mechanism could allow the ionic and electronic parts of the conductivity to separate. With regard to the the cobalt spinel, the high value of conductivity of the pristine compound (8×10^{-3} S/cm) is mainly due to the electronic part and not the ionic one since the lithium insertion does not improve this value.

The electrochemical behavior of these compounds was previously studied.[24] A better specific capacity for $Cu_2CoSn_3S_8$ (12 Li per formula or 403 mAh/g) compared to $Cu_2FeSn_3S_8$ (8 Li per formula or 273 mAh/g) was observed. Both discharges curves show a potential reduction close to 1.4 V/Li up to 6 and 8 lithium per mole for iron and cobalt spinels, respectively. Regarding the reduction process between 0 and 2 Li per formula the reduction is associated with an extraction of copper atoms.[10] For the iron compound, this latter reduction gives rise to a migration of iron atoms.[15] According to the ^{119}Sn MS results, above 2 Li per formula, the reduction step can be attributed to the complex and simultaneous tin reduction. Concerning the electrochemical cycleability, these compounds show a poor reversibility i.e., a charge/discharge ratio close to 25%, indicating an irreversible reduction process.

(24) Lavela, P.; Perez Vicente, C.; Tirado, J. L.; Branci, C.; Olivier-Fourcade, J.; Jumas, J. C. *Chem. Mater.* **1999**, submitted for publication.

Conclusion

Taking into account the results of this study obtained from Mössbauer, X-ray absorption analyses, and previous studies, an insertion process can be proposed. The framework accommodates the inserted lithium in the following way:

(i) A partial reduction of copper atoms occurs between 0 and 2 Li per formula. To check accurately the copper environment in the lithiated samples, some NMR and Rietveld analyses are planned.

(ii) No reduction of cobalt and iron atoms was observed. Nevertheless, a migration of iron atoms (Fe^{II}(16c) → Fe^{II}(8a)) occurs associated with the copper extraction.

(iii) A complex and simultaneous reduction of tin atoms Sn(IV) → Sn(II), Sn(0) is observed by ^{119}Sn MS. This process is mainly irreversible.

(iv) Concerning the sulfur environment some modifications are observed by X-ray absorption at the sulfur K-edge. These modifications can be explained by the formation of interactions between the lithium and the sulfur atoms.

With regard to the electrochemical behavior, the specific capacity of both compounds can be improved as previously reported[18,24] by the substitution of tin by titanium atoms. Finally, these compounds are rather interesting materials for a better understanding of the complex lithium intercalation process.

Acknowledgment. The authors thank A. M. Flank and P. Lagarde for their contributions in collecting data of Super-Aco at LURE (Orsay, France). The authors acknowledge the financial support PICS 505-CNRS.

CM991049A